Downlink MIMO Multiuser Detection with Interference Subspace Rejection[1]

Henrik HANSEN, Sofiène AFFES and Paul MERMELSTEIN
INRS-Télécommunications, Université du Québec
Place Bonaventure, 800, de la Gauchetière Ouest, Suite 6900
Montréal, Québec, H5A 1K6, Canada

***Abstract*— We proposed recently a new technique for multiuser detection in CDMA networks, denoted Interference Subspace Rejection (ISR), and evaluated its performance on the uplink. This paper extends its application to the Downlink (DL). On the DL the information about interference is sparse, e.g., Spreading Factor (SF) and modulation of interferers may not be known, which makes the task much more challenging. We present three new ISR variants which require no prior knowledge of the interfering users. The new solutions are applicable to MIMO systems and can accommodate any modulation, coding, spreading factor, and connection type. A new Dynamic power-Assisted Channelization Code Allocation (DACCA) technique significantly reduces implementation complexity at the receiving mobile. Simulations under practically reasonable conditions suggest that increased user capacities and data-rates are attainable with Downlink Interference Subspace Rejection (DLISR) and system capacity increases linearly with the number of antennas. Capacity gains are at least 3 dB over the single-user detector and increase to 8 dB for high data-rates with 16-QAM.**

I. Introduction

MIMO [1] and Multiuser Detection (MUD) [2]-[4] are both very promising techniques for high capacity on the downlink in wireless systems. We propose a new class of MUD solutions for DL multi-cellular interference-limited CDMA based MIMO systems. These new solutions are all DL variants of a previously presented Interference Subspace Rejection (ISR) technique [5] and are therefore referred to as DLISR. DLISR is invariant to coding, spreading, modulation and connection type (CS/PS). DLISR takes advantage of a new concept we denote Virtual Interference Rejection (VIR) combined with a new Orthogonal Variable Spreading Factor (OVSF) [6] code allocation scheme denoted Dynamic power-Assisted Channelization Code Allocation (DACCA). VIR and DACCA improve performance and most importantly reduce complexity tremendously.

Our simulations employ a very precise model of the DL transmission environment. The interference is generated by a Radio Network Simulator (RNS) and used in the link-level DLISR detector. Our solution consistently provides an Erlang capacity gain of 3 dB and more over the single user detector, and always outperforms the PIC with comparable complexity.

II. Review of Interference Subspace Rejection

A. Signal Model

Due to lack of space, we provide here a simplified and concise formulation of ISR. A more complete discussion can be found in [7]. We assume synchronous transmission, single antenna reception ($M_R = 1$), and non-selective fading. These assumptions are relaxed in the system actually simulated. However, they significantly simplify our notation and lead to improved understanding. We emphasize that in the simulated system we consider a MIMO channel structure with multiple transmit and receive antennas (M_T and M_R, respectively). Details regarding the MIMO system are found in [7]. First we present our simplified signal model; then, we present ISR.

Consider the following baseband observation vector containing contributions from Q targeted symbols (we also omit frame index n to simplify our notation):

$$\underline{\mathrm{Y}} = \psi_k^d b_k^d \underline{\mathrm{Y}}_k^d + \underline{\mathrm{I}}_k^d + \sum_{i=1}^{NI} \underline{\mathrm{I}}^i + \sum_{\nu=1}^{N_{\mathrm{HO}}} \underline{\mathrm{Y}}_\pi^\nu + \underline{\mathrm{N}} \ , \qquad (1)$$

where the terms on the right-hand side are the desired terms, the ISI, the MAI, the pilots, and the noise, respectively. Furthermore, d denotes the desired user, $i = 1, \ldots, NI$ denotes one of NI interferers, $\underline{\mathrm{Y}}_k^d$ is the unit-norm signature of the desired user (i.e., code-channel response), ψ_k^d is the amplitude, and b_k^d is the data symbol (e.g., QPSK), $k = 0, \ldots, Q-1$ is the symbol index, N_{HO} is the number of cells in the handover list, and $\underline{\mathrm{N}}$ is the AWGN due to the interference from all other active users received sufficiently weakly that it can be represented as additive white noise. The dimension of the observation is $M_R QL$, where L is the Spreading Factor (SF). We omit further details regarding the pilot and ISI. Instead we focus on the more important MAI term. The MAI interference vector, which arrives from one of the N_{HO} cells, is composed as follows[2]:

$$\underline{\mathrm{I}}^i = \sum_{k=0}^{Q-1} \psi_k^i b_k^i \underline{\mathrm{Y}}_k^i \ , \qquad (2)$$

where $\underline{\mathrm{Y}}_k^i$ is the unit norm signature defined as

$$\underline{\mathrm{Y}}_k^i = h_k^{\nu_i} \underline{\mathrm{c}}_k^i = h_k^{\nu_i} \underline{\mathrm{c}}_{\mathrm{sc},k}^{\nu_i} \circ \underline{\mathrm{c}}_{\mathrm{ch},k}^i \ , \qquad (3)$$

where ν_i is the serving cell of interferer i, $h_k^{\nu_i}$ is the channel response of the serving cell, $\underline{\mathrm{c}}_{\mathrm{sc},k}^{\nu_i}$ is the a PN scrambling code of server ν_i, $\underline{\mathrm{c}}_{\mathrm{ch},k}^i$ is a time-shifted channelization code drawn from an OVSF tree, and $\circ$ means element-wise multiplication. Please refer to [8] for more information on OVSF design. For instance, refer to the OVSF tree in Fig. 1-a (and disregard everything else). The interferer i has one of the $L = 8$ channelization codes assigned, say $\underline{\mathrm{c}}_{\mathrm{ch}}^i(L, c_{\#}^i)$ where $c_{\#}^i = 1, \ldots, L$ is one of the L available codes, then $\underline{\mathrm{c}}_{\mathrm{ch},k}^i$ arrives by delaying this code by kT where T is the symbol duration.

B. ISR Data Combining

The single user detector often employs Maximal Ratio Combining (MRC[3]). The MRC combined signal is obtained as

[1] *The work reported here was supported by the Bell/Nortel/NSERC Industrial Research Chair in Personal Communications and by the NSERC Research Grants program.*

[2] ISI $\underline{\mathrm{I}}_k^d$ is defined accordingly but the k-th index is removed from the sum.

[3] Or equivalently, matched filter combining.

$\hat{\underline{Y}}_k^{d\ H}\underline{Y}$. The MRC beamformer $\hat{\underline{Y}}_k^d$ provides only the statistical reduction of the MAI (i.e., reduction by the processing gain). The ISR beamformer, however, strives to reduce the MAI by linearly constrained beamforming. It uses a constraint matrix $\hat{\mathbf{C}}$ that attempts to span the MAI. The ISR beamformer is computed as follows:

$$\underline{W}_k = \mathbf{\Pi}\hat{\underline{Y}}_k^d/(\hat{\underline{Y}}_k^{d\ H}\mathbf{\Pi}\hat{\underline{Y}}_k^d), \quad \mathbf{\Pi}=\mathbf{I}_{QL}-\hat{\mathbf{C}}\left(\hat{\mathbf{C}}^H\hat{\mathbf{C}}\right)^{-1}\hat{\mathbf{C}}^H, \quad (4)$$

where $\mathbf{I}_{QL}$ is the QL-dimensional identity matrix, $(\cdot)^H$ means hermitian, and $\hat{\underline{Y}}_k^d$ is an estimate of the desired term. The ISR beamformer provides a unit response towards the desired term, $\hat{\underline{Y}}_k^d$, and at the same time rejects the subspace spanned by $\hat{\mathbf{C}}$. A number of different definitions are available for the ISR constraint matrix $\hat{\mathbf{C}}$, with differences in complexity and performance. Strategies for constructing $\hat{\mathbf{C}}$, referred to as modes, can be found in [5].

We consider here the Realizations mode (ISR-R) and the Hypothesized mode (ISR-H). The constraint matrices are respectively composed as follows:

$$\text{R:}\,\hat{\mathbf{C}}=\left[\hat{\underline{I}}^1,\ldots,\hat{\underline{I}}^{NI}\right],\ \text{H:}\,\hat{\mathbf{C}}=\left[\hat{\underline{Y}}_1^{i=1},\ldots,\hat{\underline{Y}}_Q^1,\hat{\underline{Y}}_1^2,\ldots,\hat{\underline{Y}}_Q^{NI}\right]. \quad (5)$$

With ISR-R we attempt to reconstruct each interfering interference vector $\hat{\underline{I}}^i$. This requires estimates of the channel response and tentative symbol decisions obtained from MRC. ISR hence uses Decision Feedback (DF). ISR-H does not require DF because it rejects each symbol signature $\hat{\underline{Y}}_k^i$ independently and any scaling of its columns will not change the result (Eq. 4). In practice we wish to cancel only the stronger interferers. In this case only columns corresponding to the targeted interferers are included. We now present DACCA and VIR. Then we will revert to ISR and propose new DLISR variants.

III. DACCA

We propose a strategy for channelization Code Allocation (CA) of user data channels at the base station, which we denote Dynamic power-Assisted Channelization-Code Allocation (DACCA). With DACCA the base station dynamically reassigns channelization codes to the users at a low rate. The code assignment is based only on the ratio between each user's output power and SF, denoted the PSFR (Power-SF Ratio) in the following. DACCA is illustrated in Fig. 1-a: The goal is to fill the OVSF tree from left to right subject to the PSFR of users. The desired outcome is a concentration of power at the left-hand side of the OVSF tree. Fig. 2 shows the relative power of the interferers arriving at a typical mobile from different sources in a network. The distributions were obtained with the RNS [7] at a Processing Gain of 16 and an offered traffic of $T_{OFF} = 4$ Erl. We observe that most of the interference is generated by just a few users. 30% of the total interference arrives from the strongest in-cell interferer and the sum of only two interferers accounts for almost half the interference. With DACCA, therefore, most of the interference power can be concentrated in a relatively small portion of the OVSF code space. This property of DACCA is valuable when combined with VIR as explained in Sec. IV.

Dynamic code assignment and reassignment strategies have previously been considered in [9], [10]. DACCA is similar to the strategy denoted 'leftmost' in [10], namely users are assigned to the leftmost available code in the OVSF tree. DACCA imposes additional restrictions because it both strives to assign the leftmost codes and at the same time to achieve the best possible concentration of power at the left-hand side of the OVSF tree. Therefore DACCA will exacerbate the probability of code-blocking. Our studies show that this is of little significance under practical conditions. DACCA does not conflict with 3G standards because channelization codes can be allocated almost freely by UTRAN[4].

IV. Virtual Interference Rejection (VIR)

Virtual Interference Rejection (VIR) can be understood by recalling that any interfering signal can be viewed as opearting at a lower SF. Define $L_R \le L$ as the Rejection Spreading Factor (RSF) and define $\gamma_L = L/L_R$, then

$$\underline{Y}_k^i = h_k^{\nu_i}\underline{c}_{\text{sc},k}^{\nu_i}\underline{c}_{\text{ch},k}^i = h_k^{\nu_i}\underline{c}_{\text{sc},k}^{\nu_i}\circ\sum_{l=0}^{\gamma_L-1} q_l\underline{c}_{\text{ch}}(L_R,\lfloor c_{\#}^i/L_R\rfloor)\text{D}^{lL/\gamma_L}, \quad (6)$$

where $q_l = \pm 1$ is the sequence that uniquely identifies the physical code from the virtual lower SF OVSF code, and D^x symbolizes a delay of x chip durations. Hence we can write the interferer as

$$\underline{I}^i = \sum_{k'=0}^{\gamma_L Q-1}\psi_k\tilde{b}_{k'}^i h_k^{\nu_i}\sum\underline{c}_{\text{sc},k}^{\nu_i}\circ\underline{c}_{\text{ch}}(L_R,\lfloor c_{\#}^i/L_R\rfloor)\text{D}^{k'L/\gamma_L}, \quad (7)$$

where $k = \lfloor k'/\gamma_L\rfloor$, and $\tilde{b}_{k'}^i = q_l b_k^i$, $l = k' - \gamma_L\lfloor k'/\gamma_L\rfloor$ has the form of a generalized data sequence. A user operating at a SF L can therefore be regarded as a virtual user operating at a lower SF, namely L_R. Note that the virtual rate is higher, but off course the information rate is unchanged. It follows that we can reject interference targeting a low RSF and, if our rejection strategy is invariant to modulation, reject more interferers simultaneously, provided that the rejected virtual code is an ancestor to the physical codes. As an example, consider the segment of an OVSF tree starting at an SF of $L = 8$ shown in Fig. 1-b. Codes that are circled are in active use. By rejecting the virtual user code $\underline{c}_{\text{ch}}(8,1)$, marked with an 'x', copied and delayed $0, 8, 16$, and 32 chip durations, all its circled descendants are rejected. Note that the code $\underline{c}_{\text{ch}}(64,8)$ is rejected although it is not active. Cancellation of inactive successor codes is a consequence of using VIR. However, ISR is much more robust to noise than PIC [11] because it employs nulling instead of subtraction.

The efficiency of VIR increases when combined with DACCA. DACCA attempts to concentrate energy in the left hand side of the OVSF tree and therefore minimizes the number of inactive codes rejected. Cancelling the leftmost code at any RSF ideally causes the highest possible fraction of the interference to be rejected when DACCA is employed. The efficiency of VIR is, therefore, enhanced when DACCA is used. If DACCA is not employed, the RSF must be higher

[4]Only the Primary CPICH and the Primary CCPCH have predefined channelization codes [8].

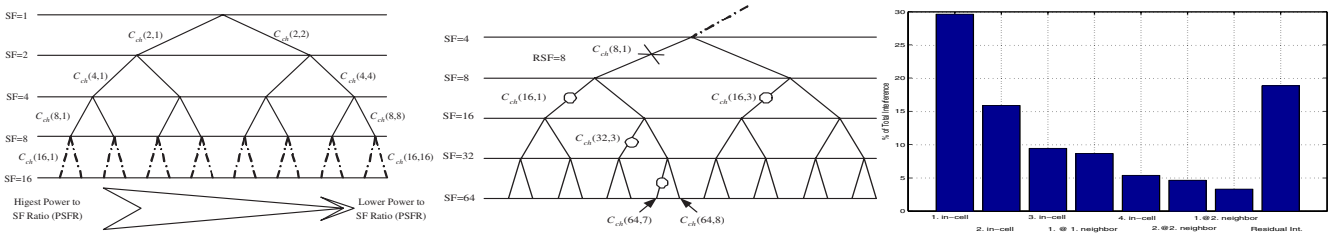

(a) (b)

Fig. 1. DACCA and VIR Illustrated. (a): In DACCA users are assigned channelization codes according to their RSFR. (b): Interference rejection is aimed at a low SF when VIR is employed.

Fig. 2. Relative power of interferers and their origin. 1 in-cell is the strongest in-cell interferer, 1@1 neighbor is the strongest interference from first-tier neighbors.

TABLE I
IN-CELL INTERFERENCE REDUCTION ESTIMATED WITH DIFFERENT RSFS
(IT IS ASSUMED THAT $3L_R/8$ CODES ARE REJECTED)

L_R (RSF)	Codes Rej.	Random	Leftmost	DACCA
8	3	3.5 dB	7.8 dB	9.4 dB
16	6	4.2 dB	8.3 dB	9.4 dB
32	12	5.1 dB	8.7 dB	9.4 dB
64	24	6.2 dB	9.0 dB	9.4 dB
128	48	7.7 dB	9.2dB	9.4 dB

to minimize the number of rejected inactive codes. In Tab. I we show the fraction of the total interference accumulated when choosing the $3L_R/8$ (e.g., 6 codes for $L_R = 16$) virtual codes that contain most interference. The code-allocation simulation assumed that the (average) carried traffic load was 50% (Poisson distributed), and a user was assigned SF $L = 8$ with probability p, $L = 16$ with $2p$, $L = 32$ with $4p$ etc. up to $16p$ for $L = 256$. The output power per symbol was drawn from an experimental output power PDF obtained by extensive simulations with the RNS. Clearly, DACCA is very efficient in concentrating interference and does that at a very low RSF. To cancel the same cumulative interference with the traditional CA schemes, we must operate at much higher RSF. Accepting a loss margin of 1 dB, we must use an RSF of at least 32 for the left-most strategy and more than 128 with random allocation. DACCA therefore allows for operation with very low RSF. This reduces complexity significantly as will be discussed later. Reducing RSF below 8 reduces complexity minimally. Moreover, accurate targeting of interference is more difficult, for instance, we can only reject 0% or 50% of the code-space if $L_R = 2$. The RSF should therefore not be lower than 8.

V. ISR VARIANTS FOR THE DL (DLISR)

DL MUD is characterized by a lack of information regarding the interferences. A mobile generally has no knowledge of the interfering users' codes, modulation, connection type, and coding. This information is only available for the pilots and the desired signal. In practice the pilots and the desired signal are easy to reject with a very simple ISR mode referred to as the Total Realization (TR) mode [5]. The MAI is, however, more challenging to remove due the sparse knowledge of interference, and only the rejection of MAI is considered in the following.

There are two ways of exploiting ISR to satisfy these limitations. ISR-H is readily applicable because it rejects interference regardless of its modulation, coding and connection type. Earlier we studied DF modes of ISR [5] assuming hard-decision FB. They cannot easily be used since modulation is not necessarily known and not well-defined (contributions from many users with offspring from the rejected virtual code). If we employ soft-decision FB this information is obsolete. It it obvious that VIR can be employed for both situations. We note that in some situations the modulation of interfering users may be known (e.g., common WCDMA radio access bearers, excluding the HSDPA technology) and Hard-Decision FB is made possible because VIR preserves modulation. However, the signal constellation is a complex combination of interfering users signal modulation constellation points, powers, and channel responses. Hard-Decision FB is therefore a more complicated solution for downlink application, and is therefore not considered here.

A. New DLISR Variants

We consider 3 new DLISR variants and PIC-SD. Important properties of these variants are summarized in Tab. II.

1) DLISR-H-FC: DLISR-H-FC is the simplest of all variants. The idea is to blindly reject the same virtual OVSF code-subspace according to a fixed strategy. Obviously, this mode is relevant only when DACCA is employed.

When employing the H-mode, interference is nearly perfectly rejected when channel identification is good [7]. But the white noise is enhanced. It can be shown [7] that the noise enhancement is given by:

$$\kappa \simeq \frac{L_R \cdot M_R - 2}{L_R \cdot M_R - 2 - N_v} \ , \tag{8}$$

where N_v is the number of virtual OVSF codes we strive to reject and L_R is the RSF. The best strategy is the optimal trade-off between noise enhancement and interference rejection. Using the RNS, the interference can be recorded (origin and strength) and a statistical ranking can be generated. From the statistical expectations the best global strategy can be derived. One strategy could be to reject two in-cell virtual codes and one code from the strongest neighbor.

2) DLISR-H-BC: In the DLISR-H-BC variant we estimate the power in the virtual subspace of the serving cell and all cells in the neighbor list. The power is estimated subject to the RSF which may represent many virtual users. Instead of relying on the statistical expected origin of interference like DLISR-H-FC this mode probes the power contained in the virtual codes of the RSF and derives the best trade-off between reduction of interference and noise enhancement (Eq. 8). Hence, this variant adapts to fast fading and will attempt to reject interference most efficiently.

3) DLISR-R-SD: In this variant we reconstruct the virtual users using soft-decision. Working at a low RSF, the N_v OVSF virtual codes which contain the most power are selected. These

TABLE II
IMPORTANT CHARACTERISTICS OF NEW ISR VARIANTS FOR DL MIMO.

Feature Strategy	Requires DACCA?	Know Int. Codes?	Know Int. SF?	Know Int. Modulation?	Applicable to PS/CS Int.?	Know Int. Coding?
ISR-H-FC	Yes	No	No	No	Yes	No
ISR-H-BC	No[1,2]	No	No	No	Yes[3]	No
ISR-R-SD	No[1,2]	No	No	No	Yes[3]	No
MRC	No	No	No	No	Yes	No

[1]: Performance gain with DACCA. [2]: Complexity reduction with DACCA. [3]: Possible performance penalty for PS.

codes are reconstructed as virtual users' signals using SD estimates based on MRC.

4) PIC-SD: As a benchmark, we will also consider PIC with SD FB. We follow the same steps as for DLISR-R-SD, except that the reconstructed interference is subtracted rather than nulled.

VI. SYSTEM-LEVEL SIMULATIONS

The simulation model is based on a Radio Network Simulator [7] followed by a link-level simulator which implements either of the proposed DLISR structures, PIC-SD, or MRC. The purpose of the RNS is to provide a realistic realization of the interference by defining a model cellular radio network and sufficiently populating it with users so that their SINR just satisfies a target operating point and block those that cannot achieve the targeted SINR either due to coverage or interference limitations. We denote the probability of blocking as the Soft-Blocking Rate (SBR). The RNS realizations of the interference are used in the link-level simulator to obtain system-level results. The RNS is most important on the DL where near-far situations are pronounced.

A. Simulation Setup

We consider a homogeneous hexagonal grid of 3-sector sites for the RNS. Sites have 3-sectors with pointing directions of $0, 120, 240^\circ$ azimuth respectively. The propagation exponent is 4. For the link-level simulations we consider low SF operation and high-order modulation schemes. We explicitly generate signals from the serving cell and the three strongest neighbors[5], whereas the interference from the remaining cells is modelled as AWGN. We employ closed-loop, fast power control. Every parameter is estimated as needed in the receiver and nothing is assumed known a priori. We use a modification [7] of STAR [12] to estimate the channels. DACCA is used with code reallocation at 75 Hz. It is further assumed that DLISR-H-BC updates its constraints at a rate of 300 Hz. Working at an RSF of 8, we found that $N_v = 2M_R$ is a good rule for good performance for DLISR-R-SD in the operating region of interest (about 5% BER). The PIC-SD interestingly shows strong sensitivity to this parameter and the best choice proves to be $N_v = M_R$. Other parameters utilized in the simulations[6], unless otherwise is specified, are summarized in Tab. III.

TABLE III
PARAMETERS USED IN SIMULATIONS.

Parameter	Value	Comment
Cell layout	Hexagonal grid, 3 sector sites	
Site to site distance	$250\sqrt{3}\ m$	
Antenna pattern	Kathrein 742212	6° electrical tilt
Antenna heights	20 m	
SBR	20%	coverage+int. blocking
CPICH power	10%	
Propagation model	Constant + $40\log_{10}(\sqrt{x^2+y^2})$	
LNF standard deviation	8 dB	
R_c	3.84 Mcps	chip rate
P	3	Equal strength paths
f_c	1.9 GHz	carrier frequency
f_D	8.9 Hz	Doppler frequency (*i.e.*, 5 Kmph)
L	8	SF
f_{PC}	1600 Hz	frequency of PC updating
ΔP_{PC}	± 1 dB	PC adjustment
BER_{PC}	10%	simulated PC bit error rate
$\frac{\delta\tau}{\delta t}T_c$	2 ppm	symbol clock drift (linear)
$\Delta\tau$	10 chips	maximal delay spread
f_{DACCA}	75 Hz	DACCA reassignment rate

B. SISO with QPSK Modulation

We consider first a Single-Input Single-Output SISO system with QPSK modulation. The SBR is 20%[7] and the SF is 8. Fig. 3-a shows the uncoded BER as a function of the carried traffic in the network. Our proposed DLISR variants significantly outperform MRC. They provide Erlang capacity gains of 3.5 dB (DLISR-H-BC) > 3.2 dB (DLISR-R-SD) > 1.6 dB (DLISR-H-FC), respectively, over the MRC at 5% BER. DLISR-H-BC achieves superior DL performance due to its pronounced near-far resistance[8]. Although PIC-SD is similar to DLISR-R-SD, it can only offer a gain of 2.6 dB. This illustrates the advantage of linearly constrained beamforming compared to subtraction[9]. With DLISR-H-BC we achieve a spectral efficiency of 0.78 bits/sec/Hz where we have defined spectral efficiency as $\eta_S = \log_2(M_{MOD})\,T_{Erl}/L$, where M_{MOD} is the number of bits per symbol for the modulation used, and T_{Erl} is the carried Erlang traffic[10] (found at 5% BER).

Comparing the attainable traffic at lower BER levels, as is often done in literature, benefits the proposed DLISR MUD. However, our internal studies have shown that 5% is an appropriate target if a rate-1/2 convolutional code with constraint length 9 is assumed. To get sound results we therefore continue to aim at 5%.

C. 2×2 MIMO with QPSK Modulation

We now consider a 2×2 MIMO system. The SF is still 8 but the PG is 16 because of the additional antenna. To allow for traffic greater than the SF we used space-time coding as described in [7]. Curves are shown in Fig. 3-b.

MRC and ISR solutions, except DLISR-H-FC, achieve a capacity gain of about 3.9 dB over SISO, whereas the MIMO gain is lower for PIC-SD. About 3 dB of these gains are due to the antenna gain. The rest is a combination of diversity and statistical multiplexing gain on the air interface. DLISR-H-FC improves more by achieving a gain of about 5 dB compared to SISO. DLISR-H-FC experiences a statistical gain because

[5]Simulations with the RNS show that the cells not generated account for less than 5% of the interference power when the traffic is 1.6 Erlangs. This number reduces further with higher traffic loads.

[6]In the absence of power control (PC), the received power ψ^2 has a χ^2 distribution with std $\sigma_{\psi^2} = 1/\sqrt{M_T \times M_R}$ that asymptotically approaches the AWGN-channel at a very high diversity order $M_T \times M_R \leftarrow \infty$. With PC (see Tab. III), however, ψ^2 has a log-Normal distribution with much weaker std that quickly approaches the AWGN-channel with few antenna elements only, as shown in [13]. Hence, PC significantly increases capacity and reduces the MIMO-array size. Indeed, as noted in [13], if we apply the asymptotic expression for the BER in the absence of PC $\mathrm{Prob}[\hat{b} \neq b] = (E_b/N_0)^{-1/M_T \times M_R} = (E_b/N_0)^{-1/\sigma^2_{\psi^2}}$ to the case of active PC (as an approximation), we may expect to obtain (from std measurements) the same capacity with PC and 3×2 antennas as would be obtained without PC and 30×2 antennas!

[7]This value may appear high when compared to, e.g., speech services, but we consider here high data-rate transmissions.

[8]On the uplink DF modes outperform the H-mode because near-far situations are less severe [5].

[9]Note the similarity of these two: With PIC interference is reconstructed and subtracted. With DLISR-R-SD the reconstructed interference is nulled.

[10]Here defined as the offered traffic multiplied by $(1 - SBR)$.

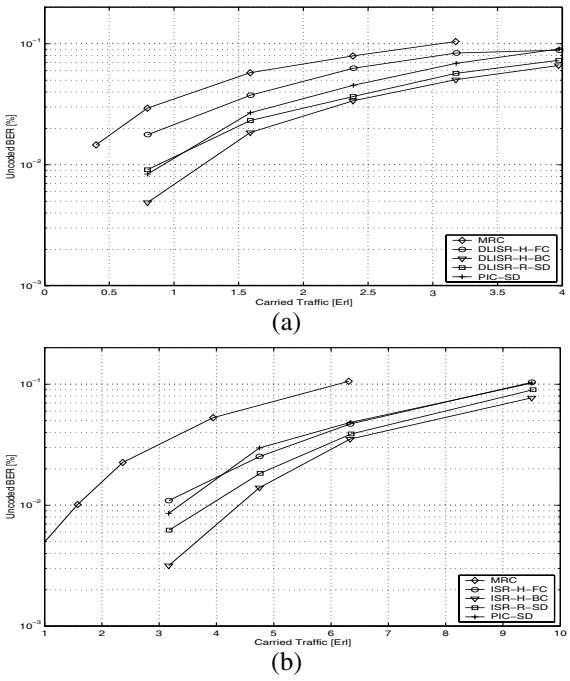

Fig. 3. Uncoded QPSK BER performance as a function of the offered traffic. The SF is 8 corresponding to an information rate of 480 kbit/s (rate-1/2 coding). (a): The channel is SISO. (b): The channel is 2×2-MIMO.

this variant uses completely fixed constraints, and interference energy is more likely to be concentrated where expected. In MIMO all DLISR variants perform better than PIC-SD except the simple DLISR-H-FC which performs equally.

The gains of our DLISR variants relative to MRC are the same as for the SISO system, expect for DLISR-H-FC which improved its performance in this situation to provide a capacity gain of 2.4 dB over MRC, closer to the 3.1 dB offered by DLISR-H-BC. The best spectral efficiency of 1.95 bits/s/Hz is again achieved by DLISR-H-BC.

D. 4×4 *MIMO with QPSK Modulation*

The number of transmit and receive antennas is now increased to 4. To allow for traffic greater than the SF we use space-time coding as described in [7]. The results are shown in Fig. 4.

The spectral efficiency of both DLISR and MRC doubles compared to the 2×2 MIMO system. We are hence able to retain our MUD advantage of more than 3 dB. PIC-SD performs as usual worse than DLISR and provides a MUD gain of only 2.1 dB. We can now support 17 Erlangs of 480 kbit/s traffic per sector corresponding to a spectral efficiency of 4 bits/Hz/sector. Comparing SISO, 2×2 MIMO, and 4×4 MIMO we notice that capacity increases linearly with the number of antennas. This linear relationship was also found for the MMSE MUD in an interference-limited cellular network [14]. In cellular interference limited systems the gain is limited to the antenna gain and is therefore mainly determined by the number of receive antennas. The number of transmit antennas serves to alleviate the shortage of OVSF codes [7].

E. 2×2 *MIMO with 16-QAM Modulation*

We use the same settings as in Sec. VI-C but consider now 16-QAM modulation corresponding to a bit rate of 960 kbit/s after rate-1/2 coding. Fig. 5-a shows the uncoded BER as a function of the carried traffic. We have used the 16-QAM symbol constellation suggested in [15].

TABLE IV
COMPLEXITY ESTIMATES OF ISR VARIANTS IN MOPS.

Variant	H-FC	H-BC	R-SD	PIC-SD	MRC	Preferred for
Total Mops @ RSF=8	1607	1753	1058	855	420	DACCA
Total Mops @ RSF=32	13728	14308	2852	1944	420	Leftmost CA

The capacity gain of DLISR compared to MRC becomes dominant offering 8.1 dB capacity increase, whereas PIC-SD as usual performs worse and offers only 6.7 dB gain over MRC. The remarkable DLISR gain over MRC results from increased data rate which effectively exacerbates the near-far situations because interference is limited to fewer sources. Compared to the QPSK results, the maximal Erlang traffic supported is reduced by about 5.4 dB for DLISR variants. The spectral efficiency, which decreases less due to the doubled symbol rate, is 1.1 bits/s/Hz for DLSIR-H-BC corresponding to reduction of 2.6 dB compared to MIMO QPSK.

Higher capacities can always be achieved at the expense of increased SBR. Increased SBR implies higher SINR operating point - even though the carried traffic is constant. To see the effect, Fig. 5-b shows performance with SBR = 60%. The spectral efficiency is increased for all modes. For instance, the DLISR-H-BC spectral efficiency is increased by 1.5 dB to yield 1.5 bits/s/Hz. This illustrates the important trade-off between capacity and network SBR. Higher SBR reduces the benefit of DLISR compared to MRC slightly - but it is still a significant 6.5 dB. MRC benefits more from increased SBR because in-cell interference becomes dominant and therefore an orthogonality gain, which is more pronounced for MRC, is achieved.

F. Discussion

Generally speaking all our new DLISR variants significantly outperform the SUD detector based on MRC. DLISR-R-SD and DLISR-H-BC always outperform PIC-SD. With QPSK modulation Erlang capacity is more than doubled. DLISR retains this advantage for SISO as well as for MIMO. Very high capacity gains of about $6.5 - 8.1$ dB are offered in situations where advanced modulation such as 16-QAM is used instead of QPSK. We have further seen that the capacity of the interference limited cellular system increases linearly with the number of receive antennas.

Complexity estimates in Mops for different RSFs are listed in Tab. IV. The operations include channel estimation with STAR [12] and each terminal is assumed to monitor two neighboring cells (see details in [7]). The complexity gains achieved with lower RSF result mainly from two factors. Higher RSF makes the task of reconstructing interference more demanding. Lower RSF makes the matrix inversion become simpler[11]. Employment of DACCA and VIR therefore reduces complexity by a factor of at least 3 (DLISR-R-SD)-8 (DLISR-H-BC), since, as argued in Sec. IV, the leftmost CA must operate at an RSF no lower than 32 (preferably higher!) to achieve the same performance. This penalty is even higher

[11]The R mode will have less columns since virtual users are effectively a combination of more users. The H-based variants will actually not change dimension but the matrix becomes more band-diagonal (if columns are arranged appropriately) and therefore complexity reduces significantly.

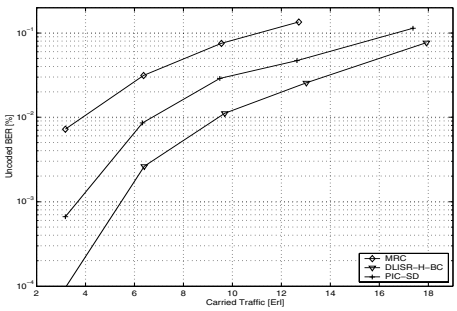

Fig. 4. Uncoded BER performance as a function of the offered traffic. The modulation is QPSK, the channel is 4×4-MIMO, and the SBR is 20%. The SF is 8.

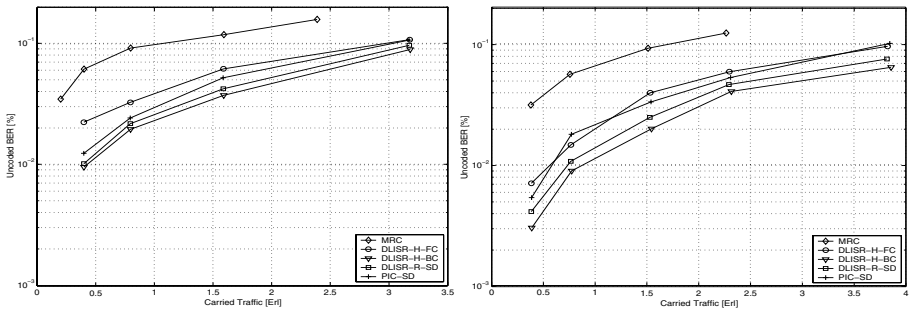

(a) (b)

Fig. 5. Uncoded BER performance as a function of the offered traffic. The modulation is 16-QAM, the channel is 2×2-MIMO, and the SF is 8 corresponding to 960 kbit/s (rate-1/2 coding assumed). (a): The SBR is 20%. (b): The SBR is 60%.

for random CA. Note that the PIC-SD does not gain much compared to DLISR-R-SD even though the latter requires a matrix inversion. This is one example of the benefit of VIR. PIC-SD has a vanishing advantage over DLISR-R-SD in terms of complexity but it does not justify its poorer performance in terms of capacity.

When DACCA is employed, the DLISR variants do not differ significantly in complexity. DLISR-H-BC consistently performs best and is therefore the preferred solution in this situation. If DACCA is not employed DLISR-H-BC and DLISR-R-SD are still applicable, but must employ higher RSF. This imposes a penalty in complexity which favor DLISR-R-SD. Since DLISR-R-SD performs nearly as well as DLISR-H-BC, the reduced complexity argues for the use of the former in this case.

VII. Conclusion

In this paper we have presented a new MUD for DL MIMO systems. Our solution is derived from previously presented Interference Subspace Rejection (ISR) and is insensitive to modulation, coding, SF, and connection type. The ISR variants share one common feature, they employ Virtual Interference Rejection (VIR) to mitigate interference at a low SF level and they benefit from dynamic allocation of channelization codes at the base station using the DACCA technique. With DACCA the base station assigns channelization codes to users according to their ratio of required output power to SF. Only one of our solutions requires DACCA. The remaining solutions benefit from DACCA because it reduces complexity.

Performance was evaluated with the aid of a realistic simulation model consisting of a radio-network simulator and a link-level simulator. The Erlang capacity of the network is found to grow linearly with the number of receive antennas for both MRC based SUD and our new DLISR MUD. Significant increases of capacity are achieved with our proposed DL MUD, namely capacity gains over MRC-based SUD of 3 dB and more for QPSK (480 kbit/s) and about $6.5 - 8.1$ dB when 16-QAM (960 kbit/s) is employed. A 4×4 MIMO system can support 17 Erlangs of 480 kbit/s traffic per sector corresponding to a spectral efficiency of 4 bits/s/Hz. PIC-SD cannot perform as well as DLSIR and its complexity is comparable, which argues against its use on the DL.

Our DLISR solution has low complexity because of VIR, especially when DACCA is employed in UTRAN. The gains cited herein are achieved at a complexity of about 1.1-1.7 Gops, which is roughly 3-4 times that of SUD. The realistic assumptions of our study suggest that our solution is low-risk. The new DLISR MUD is therefore a serious candidate for DL MUD in future CDMA-based MIMO and SISO systems.

References

[1] G. J. Foschini and M. J. Gans, "On limits of wireless communications in a fading environment when using multiple antennas," *Wireless Personal Communications*, vol. 6, pp. 311–335, March 1998.

[2] S. Verdu, *Multiuser Detection*. Cambridge University Press, 1998.

[3] A. Duel-Hallen, J. Holtzman, and Z. Zvonar, "Multiuser detection for CDMA systems," *IEEE Personal Communications*, pp. 46–58, April 1995.

[4] S. Moshavi, "Multi-user detection for DS-CDMA communications," *IEEE Communications Magazine*, pp. 124–136, October 1996.

[5] S. Affes, H. Hansen, and P. Mermelstein, "Interference subspace rejection: A framework for multiuser detection in wideband CDMA," *IEEE Journal on Selected Areas in Communications*, vol. 20, pp. 287–302, February 2002.

[6] 3GPP, "High Speed Downlink Packet Access (HSDPA) 3GPP TS 25.308 v. 5.2.0," technical specification, 3rd Generation Partnership Project, March 2002.

[7] H. Hansen, S. Affes, and P. Mermelstein, "High downlink capacity with MIMO interference subspace rejection in multicellular CDMA networks," *To appear in Eurasip J. on Applied Signal Processing Special Issue on MIMO Communications*, 1st Quarter 2003.

[8] 3GPP, "Spreading and Modulation (FDD) 3GPP TS 25.308 v. 5.2.0," technical specification, 3rd Generation Partnership Project, September 2002.

[9] T. Minn and K.-Y. Siu, "Dynamic assignment of orthogonal variable-spreading-factor codes in W-CDMA," *IEEE J. on Selected Areas in Communications*, vol. 18, pp. 1429–1440, Aug. 2000.

[10] Y.-C. Tseng, C.-M. Chao, and S.-L. Wu, "Code placement and replacementstrategies for wideband CDMA OVSF code tree management," in *IEEE GLOBECOM'01*, vol. 1, pp. 562–566, IEEE, Nov. 2001.

[11] R. Khono, H. Imai, M. Hatori, and S. Pasupathy, "Combination of an adaptive array antenna and a canceller of interference for direct-sequence spread-spectrum multiple-access system," *IEEE Journal on Selected Areas in Communications*, vol. 8, pp. 675–682, May 1990.

[12] S. Affes and P. Mermelstein, "A new receiver structure for asynchronous CDMA: STAR - the spatio-temporal array receiver," *IEEE J. on Selected Areas in Communications.*, vol. 16, pp. 1411–1422, October 1998.

[13] K. C. S. Affes, K. Lajnef and P. Mermelstein, "Adaptive mimo-diversity selection with closed-loop power control over wireless cdma rayleigh-fading channels," *IEEE/EURASIP International Symposium on Signal Processing and its Applications ISSPA'03*, July 1-4 2003.

[14] S. Catreux, P. F. Driessen, and L. J. Greenstein, "Attainable throughput of an interference-limited multiple-input multiple-output (MIMO) cellular system," *IEEE Trans. on Communications*, vol. 49, pp. 1307–1311, Aug. 2001.

[15] 3GPP, "3GPP TR 25.848 v. 4.0.0," technical specification, 3rd Generation Partnership Project, March 2001.